J Mol Model (2011) 17:2623–2630
DOI 10.1007/s00894-011-0957-z

ORIGINAL PAPER

DFT and MP2 investigations of L-proline and its hydrated complexes

Xiao-Jun Li · Zhi-Jian Zhong · Hai-Zhen Wu

Received: 30 October 2010 / Accepted: 3 January 2011 / Published online: 25 January 2011

Abstract A theoretical study of L-proline-$n$$H_2O$ (n=1–3) has been performed using the hybrid DFT-B3LYP and MP2 methods together with the 6-311++G(d,p) basis set. The results show that the P2 conformer is energetically favorable when forming a hydrated structure, and the hydration of the carboxyl group leads to the greatest stability. For hydrated complexes, the adiabatic and vertical singlet–triplet excitation energies tend to decrease with the addition of water molecules. The hydration energy indicates that in the hydrated complexes the order of stability is: binding site 2>binding site 1>binding site 3, and binding site 12>binding site 23>binding site 13. As water molecules are added, the stabilities of these hydrated structures gradually increase. In addition, an infrared frequency analysis indicated that there are some differences in the low-frequency range, which are mainly dominated by the O–H stretching or bending vibrations of different water molecules. All of these results should aid our understanding of molecular behavior and provide reference data for further studies of biological systems.

Keywords Hydrated structure · Excitation energy · Hydration energy · Infrared spectroscopy · Density functional theory (DFT) · MP2

Xiao-Jun Li and Zhi-Jian Zhong contributed equally to this work.

X.-J. Li (✉) · H.-Z. Wu
Department of Chemistry and Chemical Engineering,
Weinan Teachers University,
Weinan, Shaanxi 714000, People's Republic of China
e-mail: lixiaojun0@yahoo.com.cn

Z.-J. Zhong
Department of Arctic and Marine Biology, University of Tromsø,
Tromsø N-9037, Norway

Introduction

Recently, computer-aided investigations have provided some important contributions in the field of biological systems [1–5]. There have also been some useful works on significant molecular properties, such as the adiabatic electron affinity, the photoelectron spectrum and the hydration process [6–12]. In particular, the hydration process plays an essential role in the life sciences [13–16] and in drug design [17, 18], because it can provide insight into solvation effects such as hydrophobicities [19], surface effects [20] and solvent asymmetries [21]. Indeed, theoretical studies on the hydration process at the molecular level have already been performed [11, 12, 22–29]. For example, Ghomi et al. [23] found that the formation of a water dimer and trimer around uracil is necessary to complete the first hydration shell when using DFT calculations. Vyas et al. [26] reported that Ala-$(H_2O)_n$ complexes where water molecules are attached to the –COOH group of Ala are very stable conformers in the gas phase.

Among the various peptide and protein systems, poly L-proline II (PPII) attracts much interest as a major conformational element in aqueous solution [30]. Small proline residues have been widely investigated [31–36]. For example, Kang [36] analyzed conformational changes in Ac-Pro-NHMe using ab initio and DFT methods, and found that the population of the hydrogen-bonded conformation decreases and the population of the polyproline-like conformation increases in polar solution. However, until now there has not been a detailed study that has explored the interactions between water molecules and L-proline on the molecular scale. The hydration process is interesting as it provides an important way to analyze the features of hydrogen bonding and conformational stability, and singlet–triplet energy separation can help us to understand the

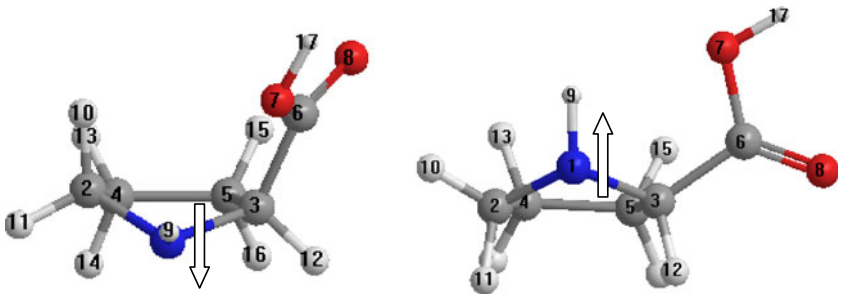

Fig. 1 The two optimized conformers obtained at the hybrid DFT–B3LYP level of theory. The relative electronic energies corrected for zero-point vibrational energy are shown in *parentheses*

damage caused to molecules by ultraviolet radiation [37, 38]. Motivated by this, we have carried out a detailed study of L-proline and its hydrated complexes using density-functional theory (DFT-B3LYP) and an ab initio method (MP2).

Computational details

All of the calculations were performed with the Gaussian 09W (version A.02) software package [39]. Becke's three-parameter hybrid exchange functional [40] with Lee, Yang, and Parr's correlation functional [41] (hereafter referred to as B3LYP) and the second-order Møller–Plesset perturbation approximation [42] (MP2) were employed in the calculations. In order to obtain reasonable computational times and accuracies, the 6-311++G(d,p) basis set [43, 44] containing diffuse and polarization functions on each atom was utilized. Harmonic vibrational calculations were also used to verify whether the optimized geometry corresponds to a molecular minimum and not to a transition state through the absence of any imaginary frequency.

The adiabatic excitation energy was evaluated as the difference between the absolute energies of the singlet and the corresponding triplet geometries in the following manner: $EE_{ad} = E(\text{optimized triplet}) - E(\text{optimized singlet})$, while the vertical excitation energy was computed as the energy difference between the optimized singlet and the corresponding triplet with the optimized singlet geometry: $EE_{vert} = E(\text{triplet energy at optimized singlet geometry}) - E(\text{optimized singlet})$. In addition, the BSSE-corrected hy-

Table 1 The phase angles (P), puckering amplitudes (Q), dipole moments, and relative energies (ΔE) of stable L-proline-nH$_2$O (n=1–3) complexes obtained at the DFT-B3LYP/6-311++G(d,p) and MP2/6-311++G(d,p) levels of theory

Structure	P (degrees)	Q (Å)	Dipole (debyes)	ΔE^a (kJ/mol)	ΔE^b (kJ/mol)
P1	228	0.35	2.63	2.32	2.90
P2	49	0.40	1.34	0.00	0.00
P1-1W-1	219	0.35	2.08	18.95	15.91
P1-1W-2	240	0.35	2.75	1.97	2.19
P1-1W-3	209	0.37	2.25	26.51	18.49
P2-1W-1	89	0.40	2.57	16.83	14.92
P2-1W-2	54	0.40	1.97	0.00	0.00
P2-1W-3	34	0.38	2.23	22.99	17.11
P1-2W-12	224	0.35	2.43	2.00	1.25
P1-2W-13	211	0.37	3.08	27.98	19.02
P1-2W-23	215	0.36	1.87	7.57	1.50
P2-2W-12	92	0.40	2.63	0.00	0.00
P2-2W-13	41	0.37	3.76	25.38	19.13
P2-2W-23	35	0.38	2.65	6.04	1.90
P1-3W-123	213	0.36	3.88	0.26	2.48
P2-3W-123	41	0.37	3.10	0.00	0.00

[a] The values were calculated at the hybrid DFT–B3LYP/6-311++G(d,p) level

[b] The values were calculated at the MP2/6-311++G(d,p) level

dration energies for stable L-proline-nH$_2$O (n=1–3) complexes were computed using the counterpoise correction method of Boys and Bernardi [45, 46].

In this study, the pseudorotation phase angle and the puckering amplitude [47] were employed to define the five-membered ring in locally stable geometries. The puckering phase angle (P) is given by:

$$\tan(P) = \frac{\theta_3 + \theta_5 - \theta_2 - \theta_4}{2\theta_1(\sin 36^\circ + \sin 72^\circ)}, \quad (1)$$

where the torsion angles θ_j are θ_1(5,3,1,2), θ_2(3,1,2,4), θ_3(1,2,4,5), θ_4(2,4,5,3), and θ_5(4,5,3,1), respectively. The puckering amplitude (Q) is calculated by the following formula: $Q^2 = 2/5\sum(\theta_j)^2$, where the puckering amplitude is in Å.

Results and discussion

Hydrated structures and relative stabilities

L-Proline has two major conformations with very similar energies (2.32 kJ mol^{-1} for the B3LYP method and 2.90 kJ mol^{-1} for the MP2 method), and the optimized geometries are shown in Fig. 1. We can see that the P2 conformer of L-proline is the lowest-energy structure. In the hydrated complexes, the numbering formalism used is as follows: 1W, 2W or 3W denotes the number of water molecules around the L-proline, and this is followed by a number (i.e., 1, 2, or 3) indicating the primary water-binding site in the molecule. The relative energies obtained at the B3LYP(or MP2)/6-311++G(d,p) theoretical level are listed in Table 1.

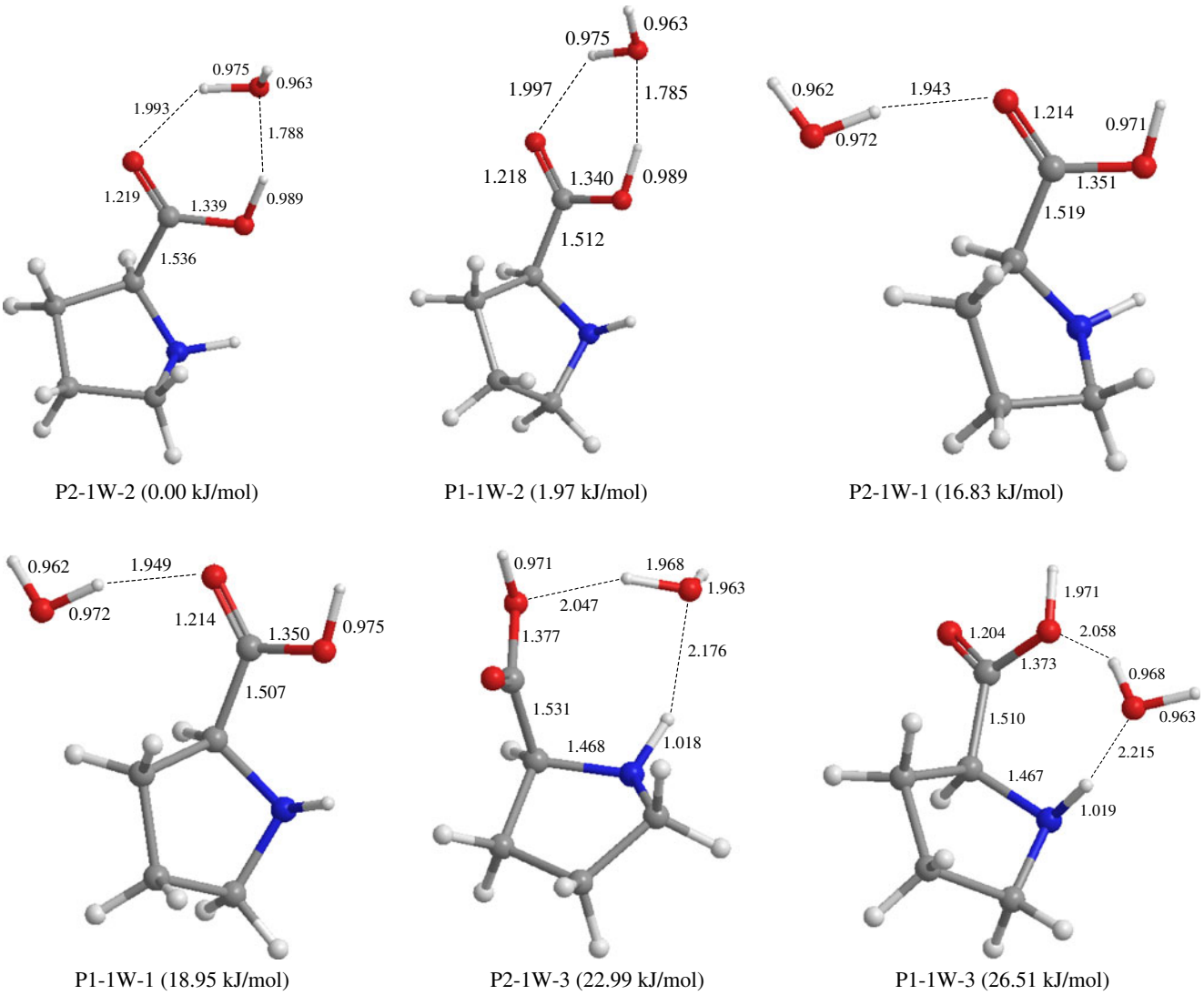

Fig. 2 Optimized geometries of six stable isomers of L-proline–H_2O complexes obtained at the hybrid DFT–B3LYP level of theory. The relative electronic energies corrected for zero-point vibrational energy are shown in *parentheses*

As can be seen from Fig. 2, six stable isomers of L-proline–H_2O complexes are obtained. The lowest-energy monohydrate structure is characterized by the O–H...O_W–H_W...O=C cyclic hydrogen bond between the P2 conformer and a water molecule. The optimized O–H...O_W and C=O... H_W hydrogen bond lengths are 1.788 and 1.993 Å, respectively. It was also found that P1-1W-2 is slightly higher in energy than the lowest-energy structure (by 1.97 kJ mol^{-1}), which is due to the fact that they have different main structure conformations. Other monohydrated structures also show that the hydrated P2 conformers are more stable than the hydrated P1 conformers, but these conformers have high energies. In particular, the three primary binding sites (P1-1W-3 and P2-1W-3) have weaker intermolecular hydrogen bonds.

Among the L-proline–$2H_2O$ complexes, P2-2W-12 (shown in Fig. 3), which possesses two water molecules at binding sites 1 and 2, is the lowest-energy structure, and this conformer has the strongest intermolecular hydrogen bond of all of the dihydrated structures. It can be obtained through the linkage of one water molecule to the lowest-energy monohydrated structure, resulting in a shorter C–O–H...O_W hydrogen bond (1.763 Å) and a longer C=O... H_W hydrogen bond (2.035 Å). As can be seen in Fig. 3, P1-2W-12 is only 2.00 kJ mol^{-1} different in energy from the lowest-energy structure. It is also clear that the binding sites 1 and 2 are more energetically favorable than sites 2 and 3 or 1 and 3. In Fig. 4, two stable conformers of L-proline–$3H_2O$ complexes are described (P1 or P2), and they show major conformational differences. We can see that P2-3W-123 is slightly lower in energy than P1-3W-123 (by 0.26 kJ mol^{-1}). The two conformers also have slightly different intermolecular hydrogen bond lengths: 1.751 (1.740) Å for the C–O–H...O_W hydrogen bond, and 2.083 (2.061) Å for the C=O...H_W hydrogen bond. In a word, the P2 conformer is energetically favored for the formation of

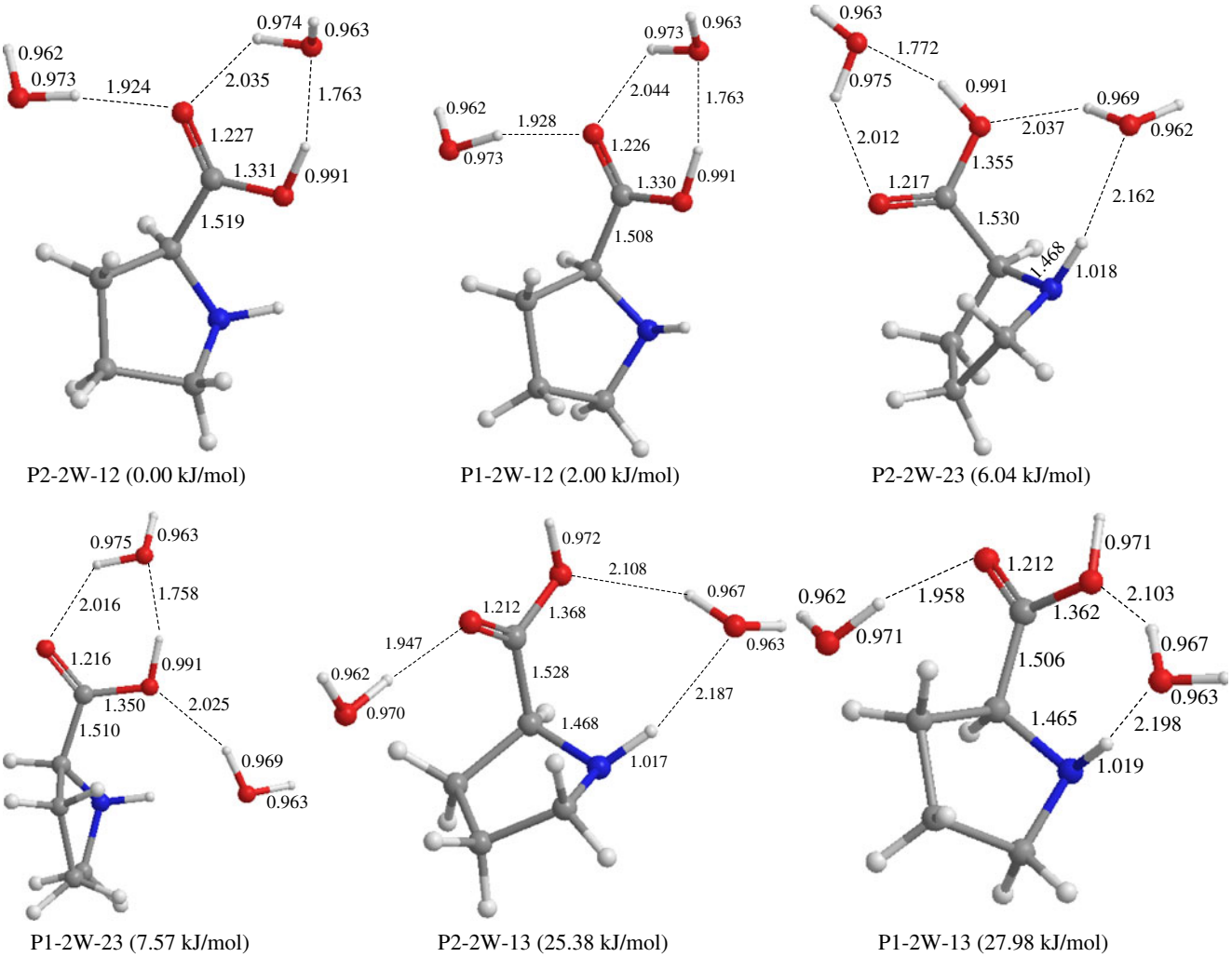

Fig. 3 Optimized geometries of six stable isomers of L-proline–$2H_2O$ complexes obtained at the hybrid DFT–B3LYP level of theory. The relative electronic energies corrected for zero-point vibrational energy are shown in *parentheses*

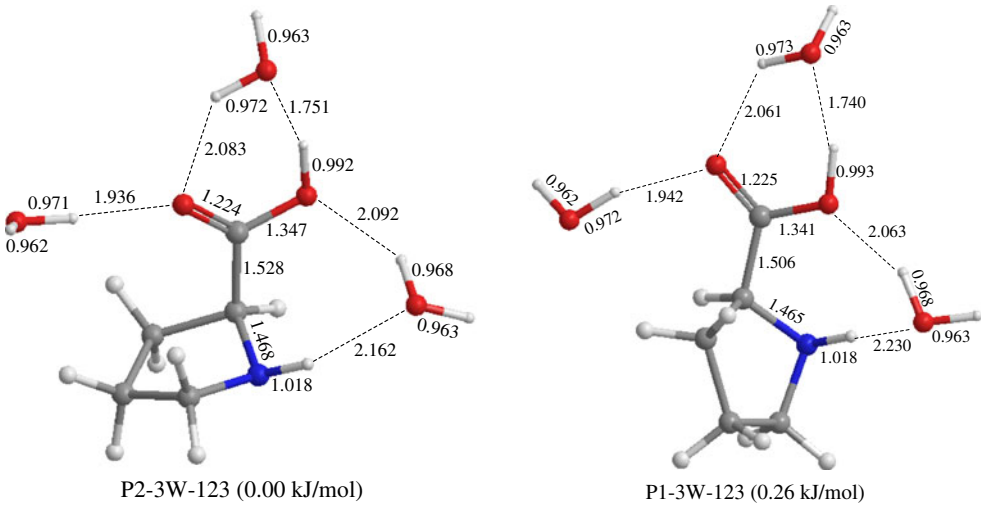

Fig. 4 Optimized geometries of two stable isomers of L-proline–$3H_2O$ complexes obtained at the hybrid DFT–B3LYP level of theory. The relative electronic energies corrected for zero-point vibrational energy are shown in *parentheses*

hydrated complexes. The order of stability of the three binding sites is 2>1>3 or 12>23>13, indicating that the hydration of the carboxyl group leads to the greatest stability, which is consistent with the results of a previous study [26]. In addition, the calculated pseudorotation phase angles and puckering amplitudes are displayed in Table 1. We can see that the phase angles are 209–240° for the hydrated P1 complexes and 34–92° for the hydrated P2

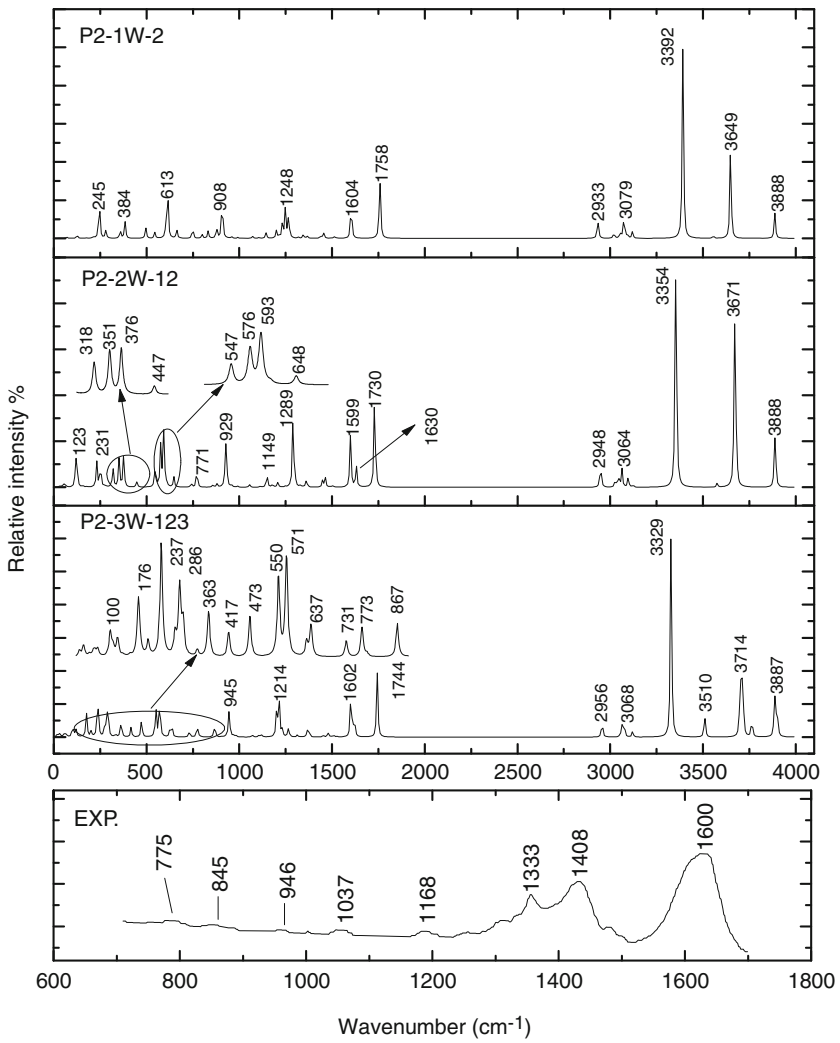

Fig. 5 Comparison of the calculated and experimental infrared spectra for hydrated L-proline complexes. The calculated spectra were obtained at the DFT-B3LYP/6-311++G(d,p) level of theory, and the experimental spectrum was reproduced from [51]

Table 2 The zero-point-corrected adiabatic excitation energies (EE_{ad}), vertical excitation energies (EE_{vert}), and zero-point- and BSSE-corrected hydration energies ($E_h^{ZPVE+BSSE}$) of stable L-proline-$n$$H_2O$ (n=1–3) complexes obtained at the DFT-B3LYP/6-311++G(d,p) level of theory

Structure	EE_{ad} (eV)	EE_{vert} (eV)	$E_h^{ZPVE+BSSE}$ (kcal/mol)
P1	3.57	5.24	–
P2	3.53	4.65	–
P1-1W-1	3.50	5.31	3.65
P1-1W-2	3.65	5.31	7.29
P1-1W-3	3.36	5.09	1.58
P2-1W-1	3.48	4.81	3.62
P2-1W-2	3.54	4.75	7.21
P2-1W-3	3.31	4.36	1.79
P1-2W-12	3.57	5.39	10.89
P1-2W-13	3.27	5.13	4.92
P1-2W-23	3.41	5.18	9.40
P2-2W-12	3.53	4.88	10.83
P2-2W-13	3.26	4.28	4.76
P2-2W-23	3.37	4.38	9.08
P1-3W-123	3.31	5.18	12.56
P2-3W-123	3.19	4.33	12.31

complexes, while their puckering amplitudes are 0.35–37 and 0.37–0.40 Å, respectively.

Excitation energies

The zero-point-corrected adiabatic excitation energies (EE_{ad}) and vertical excitation energies (EE_{vert}) of stable L-proline-$n$$H_2O$ (n=1–3) complexes obtained at the hybrid DFT–B3LYP level of theory are listed in Table 2. The hydrated P1 structures have larger adiabatic and vertical excitation energies than those of the corresponding hydrated P2 structures. In the hydrated complexes, the structures with a hydrated amine group (binding site 3) display the smallest adiabatic and vertical excitation energies, while those with a cyclic hydrated carboxyl group (binding site 2) have the largest excitation energies. The adiabatic excitation energies of P1 and P2 molecules, calculated as 3.57 and 3.53 eV, respectively, are very similar to the values of 3.6 (±0.08) eV for thymine [48], 3.5 eV for cytosine [49] and 3.65 (±0.05) eV for uracil [50], as measured using electron energy loss spectroscopy. When compared with the two free molecules, the adiabatic excitation energies of the monohydrated structures (binding site 2) are slightly higher (by 0.08 and 0.01 eV, respectively). The dihydrated structures (P1-2W-12 and the P2-2W-12) also have higher vertical excitation energies than the corresponding free molecules (by 0.15 and 0.23 eV, respectively). Moreover, we can see that, in the L-proline–$n$$H_2O$ (n=1–3) complexes, the vertical excitation energies are obviously larger than the adiabatic excitation energies (by 1.66–1.87 eV for hydrated P1 complexes and 1.01–1.35 eV for hydrated P2 complexes). The adiabatic and vertical excitation energies tend to decrease with the addition of water molecules. It is also apparent that the water molecules should have larger electron distributions in their LUMOs due to the contribution of the L-proline molecule, but the contribution of this molecule to the HOMOs of the water molecules is minor.

Hydration energies

Table 2 reports the zero-point- and BSSE-corrected hydration energies ($E_h^{ZPVE+BSSE}$) of stable L-proline–$n$$H_2O$ (n=1–3) complexes obtained using the hybrid DFT–B3LYP method. The hydration energies of the hydrated complexes can alter their relative energies. For example, the P1-3W-123 structure is more stable in hydration energy than P2-3W-123 by 0.25 kcal mol^{-1}, in contrast to their relative stabilities. As can be seen from Table 2, the monohydrated carboxyl group with an O–H...O_W–H_W...O=C cyclic hydrogen bond should be more energetically favorable than any other binding site in the P1 and P2 molecules, in accord with the results of a previous study [26]. For , P1-2W-12 (which shows binding at sites 1 and 2) has the largest hydration energy, just as it does for the excitation energies of the dihydrated complexes, as mentioned above. The hydration energy shows us that, among the hydrated complexes, the order of stability is binding site 2>inding site 1>binding site 3, and binding site 12>binding site 23>binding site 13. It should be mentioned that the stabilities of the hydrated complexes gradually increase with the addition

of water. Thus, it seems wise to explore the relative stabilities of these hydrated complexes, which depend on the number of water molecules at different binding sites. In addition, trihydrated structures have larger dipole moments, which may be due to their large hydration energies.

Harmonic vibrational frequencies

The simulated infrared spectra of the most stable L-proline–$n$$H_2O$ (n=1–3) complexes obtained at the hybrid DFT–B3LYP level of theory are shown in Fig. 5. To allow for comparison with the calculated results, the experimental infrared spectrum in the range 700–1700 cm^{-1} (as reported in [51]) is also displayed in the figure. The most stable mono-, di- and trihydrated structures have P2 as the major conformation. As can be seen in Fig. 5, the spectra of the mono-, di- and trihydrated structures all show a similar strong peak at approximately the same position: 3392, 3354, and 3329 cm^{-1}, respectively. These frequencies are mainly due to the O–H stretching vibration of the carboxyl group. With the addition of water, they are redshifted slightly by 38 and 25 cm^{-1}, respectively. In addition, the peaks at 3649 and 3888 cm^{-1} for P2-1W-2, as well as those at 3671 and 3888 cm^{-1} for P2-2W-12 and 3714 and 3887 cm^{-1} for P2-3W-123, are due to the O–H stretching vibration of the water molecule as well as its O–H bending vibration, which is similar to the results obtained experimentally [51]. Also, the peaks at 1758, 1730 and 1744 cm^{-1} can be ascribed to the O=C stretching vibration, in agreement with a previous experiment [51, 52], but the calculated infrared frequencies are redshifted by about 140 cm^{-1}. This may be due to large solvent effect in the experiment. The band at around 1600 cm^{-1}, which is mainly due to a C–H bending vibration of the pyrrolidine ring, is also consistent with the results of the corresponding experiment [52, 53]. In the three simulated infrared spectra, there are some similar profiles. However, they are still small differences at low frequencies. For example, in the dihydrated structures, the peaks at 123, 351, and 576 cm^{-1} are mostly due to the O–H stretching vibration of the water molecule located at binding site 1. In the trihydrated structure, the peaks at 176, 417 and 473 cm^{-1} are ascribed to the O–H bending vibration of the water molecule located at binding site 3.

Conclusions

In this work, we performed a theoretical study of L-proline–$n$$H_2O$ (n=1–3) complexes using density-functional theory (DFT-B3LYP) and an ab initio method (MP2). Some molecular properties were considered, such as the hydrated structures, the zero-point-corrected adiabatic excitation energies, the vertical excitation energies, the hydration energies, and infrared spectra. According to the calculated results, the P2 conformer is energetically favored for the formation of a hydrated structure, and the hydration of carboxyl group leads to the greatest stability. For hydrated complexes, the adiabatic and vertical singlet–triplet excitation energies tend to decrease with the addition of water molecules. The hydration energy shows that, in the hydrated complexes, the order of stability is: binding site 2>binding site 1>binding site 3, and binding site 12> binding site 23>binding site 13. It should be noted that, as water molecules are added, the stabilities of the hydrated complexes gradually increase. In addition, an analysis of the infrared spectra for the three most stable mono-, di- and trihydrated structures are similar in that they exhibit their strongest peaks at almost the same position in the spectrum: 3392, 3354, and 3329 cm^{-1}, respectively. However, they are still some small differences among the spectra in the low-frequency range, which is mainly dominated by the O–H stretching or bending vibrations of different water molecules. We hope that these results will provide a reference for further experimental and theoretical work in this field.

Acknowledgments This work was financially supported from the start-up fund (No.08YKZ010) of the Weinan Teachers University of China.

References

1. Deckert-Gaudig T, Rauls E, Deckert V (2010) J Phys Chem C 114:7412–7420
2. Soto-Verdugo V, Metiu H, Gwinn E (2010) J Chem Phys 132:195102(1–10)
3. Parker AW, Lin CY, George MW, Towrie M, Kuimova MK (2010) J Phys Chem B 114:3660–3667
4. Semencic MC, Heinze K, Forster C, Rapic V (2010) Eur J Inorg Chem 2010:1089–1097
5. Morera-Boado C, Mora-Diez N, Montero-Cabrera LA, Alonso-Becerra E, González-Jonte RH, de la Vega JMG (2010) J Mol Graph Model 28:604–611
6. Walch SP (2003) Chem Phys Lett 374:496–500
7. Evangelista FA, Paul A, Schaefer HF III (2004) J Phys Chem A 108:3565–3571
8. Magdalena P, Antonio R, Jerzy L (2002) J Phys Chem A 106:11008–11016
9. Mendham AP, Palmer RA, Potter BS, Dines TJ, Snowden MJ, Withnall R, Chowdhry BZ (2010) J Raman Spectrosc 41:288–302
10. Fricke H, Schwing K, Gerlach A, Unterberg C, Gerhards M (2010) Phys Chem Chem Phys 12:3511–3521
11. Clifton E, Jan S, Martin V, Nick CP (2010) J Phys Chem A 114:5919–5927
12. Rasmussen AM, Lind MC, Kim S, Schaefer HF III (2010) J Chem Theor Comput 6:930–939
13. Pocker Y (2000) Cell Mol Life Sci 57:1008–1017
14. Robertson EG, Simons JP (2001) Phys Chem Chem Phys 3:1–18
15. Chalikian TV, Macgregor RB Jr (2007) Phys Life Rev 4:91–115
16. Bowers MT, Wyttenbach H (2009) Chem Phys Lett 480:1–16

17. Pèpe G, Guiliani G, Loustalet S, Halfon P (2002) Eur J Med Chem 37:865–872
18. Klimovich PV, Mobley DL (2010) J Comput Aided Mol Des 24:307–316
19. Ashbaugh HS, Kaler EW, Paulaitis ME (1999) J Am Chem Soc 121:9243–9244
20. Chorny I, Dill KA, Jacobson MP (2005) J Phys Chem B 109:24056–24060
21. Mobley DL, Barber AE, Fennell CJ, Dill KA (2008) J Phys Chem B 112:2405–2414
22. Dybal J, Schmidt P, Kriz J, Kurkova D, Rodriguez-Cabello JC, Alonso M (2004) Macromol Symp 205:143–150
23. Gaigeot MP, Kadri C, Ghomi M (2001) J Mol Struct 565:469–473
24. Francesco T, Bencini A, Maurizio B, Luca DG, Giuseppe Z, Piercarlo F (2003) J Phys Chem A 107:1188–1196
25. Vitorino GP, Barrera GD, Mazzieri MR, Binning RC Jr, Bacelo DE (2006) Chem Phys Lett 432:538–544
26. Vyas N, Ojha AK (2010) J Mol Struct THEOCHEM 940:95–102
27. Kim HT (2004) J Mol Struct THEOCHEM 673:121–126
28. Li Q, Wang N, Yu Z (2007) J Mol Struct THEOCHEM 847:68–74
29. Mobley DL, Bayly CI, Cooper MD, Dill KA (2009) J Phys Chem B 113:4533–4537
30. Shi Z, Woody RW, Kallenbach NR (2002) Adv Protein Chem 62:163–240
31. Carlson KL, Lowe SL, Hoffmann MR, Thomasson KA (2006) J Phys Chem A 110:1925–1933
32. Che Y, Marshall GR (2006) Biopolymer 81:392–406
33. Ahmed Z, Myshakina NS, Asher SA (2009) J Phys Chem B 113:11252–11259
34. Zeng B, Shen T, Wu A, Cai S, Yu X, Xu X, Chen Z (2010) J Phys Chem A 114:5211–5216
35. Hudaky I, Perczel A (2003) J Mol Struct THEOCHEM 630:135–140
36. Kang YK (2004) J Mol Struct THEOCHEM 675:37–45
37. Pfeifer GP, You YH, Besaratinia A (2005) Mutat Res 571:19–31
38. Cadet J, Sage E, Douki T (2005) Mutat Res 571:3–17
39. Frisch MJ, Trucks GW, Schlegel HB, Scuseria GE, Robb MA, Cheeseman JR, Scalmani G, Barone V, Mennucci B, Petersson GA, Nakatsuji H, Caricato M, Li X, Hratchian HP, Izmaylov AF, Bloino J, Zheng G, Sonnenberg JL, Hada M, Ehara M, Toyota K, Fukuda R, Hasegawa J, Ishida M, Nakajima T, Honda Y, Kitao O, Nakai H, Vreven T, Montgomery JA, Peralta JE Jr, Ogliaro F, Bearpark M, Heyd JJ, Brothers E, Kudin KN, Staroverov VN, Kobayashi R, Normand J, Raghavachari K, Rendell A, Burant JC, Iyengar SS, Tomasi J, Cossi M, Rega N, Millam JM, Klene M, Knox, JE Cross JB, Bakken V, Adamo C, Jaramillo J, Gomperts R, Stratmann RE, Yazyev O, Austin AJ, Cammi R, Pomelli C, Ochterski JW, Martin RL, Morokuma K, Zakrzewski VG, Voth GA, Salvador P, Dannenberg JJ, Dapprich S, Daniels AD, Farkas O, Foresman JB, Ortiz JV, Cioslowski J, Fox DJ (2009) Gaussian 09, revision A.02. Gaussian Inc., Wallingford
40. Becke AD (1993) J Chem Phys 98:5648–5652
41. Lee C, Yang W, Parr RG (1988) Phys Rev B 37:785–789
42. Møller C, Plesset MS (1934) Phys Rev 46:618–622
43. Mclean AD, Chandler GS (1980) J Chem Phys 72:5639–5648
44. Krishnan R, Binkley JS, Seeger R, Pople JA (1980) J Chem Phys 72:650–654
45. Boys SF, Bernardi F (1970) Mol Phys 19:553–566
46. Simon S, Duran M, Dannenberg JJ (1996) J Chem Phys 105:11024–11031
47. Cremer D, Pople JA (1975) J Am Chem Soc 97:1354–1358
48. Abouaf R, Pommier J, Dunet H (2003) Chem Phys Lett 381:486–494
49. Abouaf R, Pommier J, Dunet H, Quan P, Nam PC, Nguyen MT (2004) J Chem Phys 121:11668–11674
50. Nguyen MT, Zhang R, Nam PC, Ceulemans A (2004) J Phys Chem A 108:6554–6561
51. Daněček P, Kapitán J, Baumruk V, Bednárová L, Kopecký V Jr, Bouř P (2007) J Chem Phys 126:224513(1–13)
52. Swenson CA, Formanek R (1967) J Phys Chem 71:4073–4077
53. Miller FA (1953) In: Gilman H (ed) Organic chemistry, vol 3. Wiley, New York